Diagn Interv Radiol 2023; DOI: 10.4274/dir.2022.221462

ABDOMINAL IMAGING

ORIGINAL ARTICLE

Quantitative liver magnetic resonance imaging: correlation between conventional magnetic resonance imaging, laboratory values, and prognostic indices in Budd–Chiari syndrome

Ayşe Erden
Diğdem Kuru Öz
Mehmet Adıgüzel
Funda Seher Özalp Ateş

PURPOSE

In Budd–Chiari syndrome (BCS), unevenly distributed parenchymal changes and perfusion abnormalities occur due to hepatic venous outflow obstruction. This study aimed to evaluate the changes in the liver parenchyma in BCS using the quantitative magnetic resonance (MR) techniques of MR elastography, T1 and T2 mapping, and diffusion imaging and correlate the quantitative MR parameters through biochemical results and prognostic indices.

METHODS

Fourteen patients with BCS (seven men and seven women) were examined retrospectively. Liver stiffness (kPa), T1 relaxation times (ms) were achieved using the modified Look–Locker inversion recovery (MOLLI) 3(2)3(2)5 sequence and B1-corrected variable flip angle methods, T2 relaxation times (ms), and apparent diffusion coefficient (ADC) values (mm^2/s) were measured using regions of interest placed in the same region in all quantitative methods. Measurements were repeated at the precontrast and postcontrast hepatobiliary phases. The reduction rate (RR; %) and adjusted postcontrast T1 (%) were calculated. The values obtained from different liver parenchyma areas (whole liver, caudate lobe, pathological T2 hyperintense tissue, and relatively preserved normal-appearing tissue) were compared using the Wilcoxon signed-rank test. Spearman's correlation coefficient was used to investigate the correlation between quantitative MR parameters and biochemical parameters/prognostic scores (Child–Pugh score, Clichy score, and Rotterdam index).

RESULTS

The parenchymal stiffness and precontrast T1 values of the caudate lobe were significantly lower than those of the remainder of the parenchyma, whereas the adjusted postcontrast T1 percentages (MOLLI) were significantly higher ($P \leq 0.027$). The parenchymal stiffness value, T1 and T2 values, percentages of RR (MOLLI), and adjusted postcontrast T1 values for the pathological tissue and relatively normal tissue were significantly different ($P < 0.028$). No significant difference was found in terms of ADC values between any of the distinct regions of the liver.

A strong correlation was detected between the Child–Pugh score, Clichy score, and precontrast T1 values obtained through the MOLLI sequence ($r = 0.867$, $P = 0.012$, $r = 0.821$, $P = 0.023$, respectively). No correlation was found between the whole liver stiffness values and the laboratory parameters, fibrosis markers, prognostic indices, or MR parameters. A significant correlation was identified between creatinine levels and several T1 parameters and the T2 relaxation time ($r \geq 0.661$, $P \leq 0.052$).

CONCLUSION

Tissue stiffness and T1 relaxation values are high in the areas identified as fibrosis compared with those in the relatively preserved parenchyma. The T1 relaxation time can offer quantitative information for assessing segmental functional changes and prognosis in BCS.

KEYWORDS

Budd-Chiari syndrome, diffusion weighted imaging, MR elastography, T1 mapping, T2 mapping

From the Department of Radiology (A.E., D.K.Ö. ✉ digdem_k@hotmail.com, M.A.), Ankara University Faculty of Medicine, Ankara, Turkey; Department of Biostatistics and Medical Informatics (F.S.Ö.A.), Manisa Celal Bayar University, Faculty of Medicine, Manisa, Turkey.

Received 21 February 2021; revision requested 27 March 2021; last revision received 27 August 2022; accepted 29 September 2022

Epub: 23.12.2022

Publication date: 30.05.2023

DOI: 10.4274/dir.2022.221462

You may cite this article as: Erden A, Kuru Öz D, Adıgüzel M, Özalp Ateş FS. Quantitative liver magnetic resonance imaging: correlation between conventional magnetic resonance imaging, laboratory values, and prognostic indices in Budd–Chiari syndrome. *Diagn Interv Radiol.* 2023;29(3):428-436.

Budd–Chiari syndrome (BCS) is a rare vascular disorder that develops as a result of the obstruction of hepatic venous drainage at any level between the hepatic venules and the right atrium. Liver damage in BCS is uneven, and the distribution and severity of parenchymal involvement vary according to the site and length of the venous segment involved as well as the chronicity of the disease process.[1,2]

The histological changes (congestion, loss of hepatocytes without inflammatory infiltrates, coagulative necrosis, and/or fibrosis) in BCS are not pathognomonic. Given the diagnostic effectiveness of radiologic studies such as magnetic resonance imaging (MRI), liver biopsy is not usually necessary for the diagnosis. A biopsy is only essential for confirming BCS in the case of small intrahepatic vein obstruction in the presence of preserved large veins during imaging.[3]

As a non-invasive method, conventional MRI is relatively accurate (with a sensitivity and specificity >90%) for detecting the parenchymal changes and perfusional abnormalities observed in BCS.[4] Quantitative MRI techniques such as MR elastography (MRE), T1 and T2 mapping, and apparent diffusion coefficient (ADC) measurements are known to be useful in evaluating congestive, necrotic, and fibrotic changes in the hepatic tissue.[5-7] Because the venous obstruction affects the liver in a heterogeneous way, damage to the liver parenchyma also becomes unevenly distributed.[8] To our knowledge, this uneven parenchymal involvement and the deterioration of regional and global hepatic function in BCS have not been extensively studied using MR quantification techniques.

This study aims to utilize the quantitative MR techniques of MRE, T1 and T2 mapping, and diffusion-weighted imaging (DWI) in BCS to evaluate changes in the liver parenchyma caused by hepatic venous outflow obstruction and correlate quantitative MR parameters using laboratory parameters and prognostic indices.

Main points

- T1 mapping provides absolute and comparable data that can be used to estimate the heterogeneous distribution of liver function in patients with Budd–Chiari syndrome (BCS).
- The Child–Pugh score and serum creatinine level, which are important determinants of prognosis in BCS, were correlated with the liver T1 relaxation time.
- The combined use of T1 mapping and magnetic resonance (MR) elastography is beneficial because tissues with high stiffness values on MR elastograms may be compatible with congestion if they appear relatively preserved on T1 maps.

Methods

Study participants

This study was approved by the Human Research Ethics Committee of the Faculty of Medicine, Ankara University (06/25/2021; I5-366-21), and written informed consent was waived because of the study's retrospective design. The BCS diagnosis was based on imaging findings. The data eligible for this study were obtained from patients with BCS who underwent MRE, T1 and T2 mapping, and DWI in addition to a standard unenhanced and dynamic gadoxetic-acid-enhanced liver examination.

Twenty-two MR examinations, including through quantitative techniques, performed between November 2017 and November 2021, of 14 patients with BCS (seven men, seven women; median age, 35 years; age range, 20–60 years) were reanalyzed. Of the patients who received multiple scans, only the measurements on the parametric maps of recent examinations were used for statistical evaluation. The demographic variables (known duration of disease, etiologic/predisposing factors, which veins are occluded, endovascular treatment performed, and prognostic indices) are presented in Table 1. The results of laboratory tests [including alanine transaminase and aspartate transaminase (AST), serum bilirubin, prothrombin time (PT), international normalized ratio (INR), serum albumin, platelet count, serum creatinine, and serum sodium] from the visit closest to the MRI examination were recorded. The prognostic indices for BCS (Child–Pugh score, Clichy index, and Rotterdam BCS index) were calculated. For the Child–Pugh score, five variables (serum bilirubin, albumin, INR, ascites, and hepatic encephalopathy) were scored 1–3, with 3 indicating the most severe abnormality. Based on these variables, the patients were classified into categories A to C. The Clichy index was calculated as follows: (ascites score × 0.75) + (age × 0.037) + (Child–Pugh score × 0.28) + (age × 0.037) + (creatinine × 0.0036), where ascites was scored as absent, controlled with sodium restriction or diuretics, or resistant to medical treatment (scored as 1, 2, or 3, respectively). The Rotterdam BCS index was calculated as follows: (1.27 × encephalopathy) + (1.04 × ascites) + (0.72 × PT) + (0.004 × bilirubin), where ascites and hepatic encephalopathy were scored as present (1) or absent (0) and PT as higher (1) or equal/lower (0) than an INR of 2.3.[9]

In addition, the fibrosis score of the AST to platelet ratio index was determined. As reported previously, acute disease was defined as a clinical duration of less than one month, subacute disease from one to six months, and chronic disease as longer than six months.[10] In this study, all cases were considered to be chronic BCS because the disease duration after diagnosis was longer than six months. The presence of intrahepatic collaterals, which are known to occur several months after thrombosis, in all patients also suggested the chronicity of the disease. A transjugular intrahepatic portosystemic shunt (TIPS) was performed in three of the patients. However, because we aimed to determine how the chronic parenchymal changes would be reflected when using quantitative methods, we did not exclude these patients.

Magnetic resonance image acquisition

All images were acquired using a 1.5-T MR scanner (Aera, Siemens Healthcare, Erlangen, Germany) after a 6-h fast. Standard body and spine matrix coils were used. A routine MR protocol consisting of a coronal T2-weighted half-fourier acquisition single-shot turbo spin echo, transverse T2-weighted fat-suppressed BLADE, transverse T2-weighted BLADE, and DWI were used in all patients. Gadoxetic acid (Primovist, Bayer Healthcare, Leverkusen, Germany) was administered intravenously using an automatic injector at a rate of 4 mL/s for a total dose of 0.025 mmol/kg body weight, followed by a 25-mL saline flush. After the unenhanced phase, the arterial phase (25 s), portal venous phase (60 s), delayed phase (100–120 s), transient phase (about the tenth minute), and hepatobiliary (HB) phase (about the twentieth minute) were acquired using a fat-suppressed T1 volumetric interpolated breath-hold examination sequence.

Magnetic resonance elastography

MRE was performed using a phase-contrast two-dimensional gradient recalled echo sequence. Four 10-mm-thick transverse slices through the largest cross-section of the liver were obtained with breath holds at end-expiration. The parameters used for MRE were as follows: repetition time/echo time (TR/TE): 50/27.5 ms; flip angle: 25°; field of view (FOV): 400 × 300 mm; matrix: 48 × 128, slice thickness: 10 mm; averages: 1; wave frequency: 60 Hz; motion encoding gradient frequency:

Table 1. Clinical and magnetic resonance image data of the 14 patients with Budd–Chiari syndrome

Case	Sex	Age (y)	Known duration (y)	Etiology/predisposing factor	Obstructed veins	Vascular intervention	CP class	Rotterdam score	Clichy score	CP score	APRI score
1	F	28	5	Factor V Leiden mutation (heterozygote) Protein C and S deficiency Oral contraceptive Obesity Smoking	RHV, MHV	TIPS	A	0.65	3.234	5	0.20
2	F	30	1	-*	MHV, LHV		A	0.37	3.28	5	0.28
3	M	59	1	Essential thrombocytosis	RHV, LHV, MPV		A	0.31	4.361	5	0.23
4	M	31	7	-	MHV, LHV	TIPS	B	1.91	5.19	9	1.13
5	F	32	9	Resistance to activated protein C Oral contraceptive	RHV		B	1.12	3.916	7	0.88
6	M	20	1	FMF Antiphospholipid syndrome	RHV, MHV		B	1.2	3.473	7	0.36
7	F	60	2?	Factor V Leiden mutation (heterozygote)	RHV, MHV LHV, RPV		A	0.22	4.39	5	0.40
8	M	40	10	-	RHV, MHV	TIPS	A	1.01	3.644	5	0.42
9	F	37	18	Factor V Leiden mutation (homozygote)	RHV, MHV LHV		C	0.51	5.693	10	0.74
10	M	33	3	- Smoking	RHV		A	3.07	3.396	5	0.12
11	M	45	15	- Smoking	RHV, MHV LHV		B	0.45	4.404	7	0.27
12	F	45	13	Protein C and S deficiency Factor V Leiden mutation Oral contraceptive	MHV, LHV		A	1.09	4.18	6	0.77
13	M	24	4	Factor V Leiden mutation	RHV, MHV, IVC		B	0.3	4.648	8	0.54
14	F	43	10	-	RHV		A	2.21	3.762	5	0.30

*, etiology is not determined; y, years; CP, Child–Pugh; APRI, aspartate transaminase to platelet ratio index; RHV, right hepatic vein; MHV, middle hepatic vein; LHV, left hepatic vein; MPV, main portal vein; RPV, right portal vein; IVC, inferior vena cava; FMF, familial mediterranean fever; TIPS, transjugular intrahepatic portosystemic shunt; F, female; M, male.

60 Hz; bandwidth: 250 Hz/pixel; and generalized autocalibrating partially parallel acquisitions (GRAPPA) reduction factor: 2; the scanning time of each slice was 17 s, and the total examination time was approximately 2 min, including four breath-hold and resting periods. Stiffness maps (elastograms), confidence maps, and wave images were then reconstructed using postprocessing software.

T1 mapping

A modified Look–Locker inversion recovery (MOLLI) technique was used for the precontrast (native) and contrast-enhanced T1 mapping. An electrocardiography-gated 3(2)3(2)5 sampling scheme was acquired with a balanced steady-state-free precession sequence. For T1 mapping, a single 10-mm-thick slice was taken from the same axial plane and selected for stiffness measurements in the elastogram confidence map.

The MOLLI 3(2)3(2)5 scheme was obtained with the following parameters: TR/TE: 419/1.69 ms; inversion time: 260 ms; flip angle: 50°; FOV: 390 × 313 mm; matrix: 180 × 224; slice thickness: 10 mm; fat saturation: spectral adiabatic inversion recovery (SPAIR); averages: 1; bandwidth: 603 Hz/pixel; and GRAPPA reduction factor: 2. The acquisition time was 10–20 s. Inline T1 maps were constructed at the scanner using vendor-supplied software.

A B1 inhomogeneity-corrected volumetric T1 map using a variable flip angle (VFA) method was also performed for each participant. Cardiac gating was not used for the VFA method. Multisection data (72 slices) were obtained with a breath hold of 19 s. The sequence parameters were as follows: TR/TE 4.3/2.08 ms; flip angle: 3° and 15°; FOV: 380 × 309 mm; matrix: 156 × 256; slice thickness: 3.5 mm; distance factor: 20%; averages: 3; bandwidth: 350 Hz/pixel; and controlled aliasing in volumetric parallel imaging reduction factor: 2; the acquisition time was approximately 20 s. Although multiple slices were taken during the B1-corrected volumetric T1 mapping, only one slice plane, from which the tissue stiffness was measured, was used for quantitative analysis.

T2 mapping

The T2 mapping was performed using a fast low-angle shot inversion-recovery gradient echo (FLASH) sequence with a slice thickness of 10 mm. Cardiac gating was used to time the image acquisition. Each slice had the same transverse anatomic level as in the T1 mapping. The sequence-specific parameters of the FLASH T2 mapping were as follows: TR/TE: 207/1.06 ms; flip angle: 12°; FOV: 360 × 289 mm; matrix: 116 × 192; slice thickness: 10 mm; averages: 1; bandwidth: 1184 Hz/pixel; and GRAPPA reduction factor: 2; the acquisition time was 7–12 s.

Diffusion-weighted imaging

The DWI technique was performed based on free breathing using fat-suppressed echo-planar imaging (EPI). Diffusion gradients at b values of 50, 400, and 800 s/mm^2

were used. Images were obtained with the following parameters: TR/TE: 6.700/56 ms; EPI factor: 120; bandwidth: 2.332 Hz/pixel; FOV: 380 × 90 mm; matrix size: 134 × 100; averages: 2; slice thickness: 6 mm; distance factor, 20% (1.2 mm); and GRAPPA reduction factor: 2; in addition, SPAIR fat suppression was used. The acquisition time was approximately 2.40 min.

Image analysis

The quantitative analysis of the hepatic parenchyma and T1 measurements of the spleen was performed by an experienced radiologist (D.K.Ö.) on parametric maps at a workstation (Syngo Via, Siemens Medical Systems, Erlangen, Germany).

To determine liver stiffness (kPa), T1 and T2 relaxation times (ms), and ADC values (mm^2/s), regions of interest (ROI) were placed at identical locations in each sequence, excluding large vessels and imaging artifacts. The T1 relaxation times of the liver and spleen before and 20 min after gadoxetic acid administration were measured at the same slice level of the T1 maps acquired using the MOLLI 3(2)3(2)5 sequence and B1-corrected VFA technique. Measurements were taken from the whole liver, the caudate lobe, and the rest of the liver parenchyma (excluding the caudate lobe) using the free-hand geographic ROI method. Simultaneously, the pathologic [hyperintense areas on T2-weighted images (T2WIs)] and relatively preserved (normal-appearing) areas were quantitatively assessed by drawing circular ROIs (approximately 200 mm^2). The measurements were repeated three times, and the averaged values were used for statistical analysis.

Gadoxetic acid-enhanced MRI-based liver function indices using the T1 relaxation time were calculated in the following manner, as described previously:[11]

Reduction rate (RR) of T1 relaxation time = [(T1 liver precontrast – T1 liver HB) / T1 liver precontrast] × 100

The adjusted postcontrast T1 was calculated as described by Yoon et al.[12] using the following formula:

Adjusted postcontrast T1 = (T1 liver HB – T1 spleen/T1 spleen HB) × 100

To estimate the interobserver agreement, another radiologist (M.A.) also performed measurements from the same sequences.

Statistical analysis

All statistical analyses were performed using SPSS software for Windows, version 11.5. Descriptive statistics using the median (with minimum and maximum) were performed to present the clinical characteristics of the study participants and for the quantitative MR liver name abbreviation added function parameters. The Wilcoxon signed-rank test was used to compare the results of the quantitative parameters obtained from different regions of the liver. Spearman's correlation coefficient was used to measure the strength of correlation between the quantitative MR parameters and biochemical parameters and prognostic scores, where the value r = 1 represented a strong positive correlation and the value r = –1 was a strong negative correlation. The interobserver agreement was examined using the intraclass correlation coefficient (ICC). A P of <0.050 was considered statistically significant.

Results

The venous obstruction sites of the 14 patients with BCS involved in the study are presented in Table 1.

Comparison of quantitative parameters in the caudate lobe and the rest of the liver parenchyma

The median (minimum–maximum) stiffness, T1 (MOLLI sequence and B1-corrected VFA technique), T2, and ADC values in the caudate lobe and the remainder of the liver parenchyma are shown in Table 2. The MOLLI, T1 mapping, and T2 mapping measurements were performed on 10 patients.

The caudate lobe median stiffness value was significantly lower than that of the other parts of the parenchyma (3.29 vs. 5.07 kPa, P = 0.001).

A significant difference in the precontrast MOLLI T1 relaxation time (P = 0.012), precontrast B1-corrected VFA (P = 0.006), and adjusted postcontrast T1 (P = 0.027) was identified. The T1 values obtained using both mapping techniques were significantly lower in the caudate lobe than in the other parts of the parenchyma (Table 2). The T1 RR on both the MOLLI and B1-corrected VFA images revealed no significant difference (60% vs. 59%, P = 0.172; 67% vs. 66%, P = 0.399, respectively).

In addition, no significant difference was found in terms of median T2 value (P = 0.141) or ADC value (P = 0.346) (Table 2).

Comparison of quantitative parameters in areas seen as hyperintense on T2-weighted images and the relatively preserved parenchyma

The median (minimum–maximum) stiffness, T1, T2, and ADC values in areas seen as hyperintense on the T2WIs and relatively preserved normal-appearing liver parenchyma are presented in Table 2.

The T2 hyperintense region median tissue stiffness was significantly higher than that of the relatively normal-appearing liver parenchyma (6.14 vs. 2.96 kPa, P = 0.001) (Figure 1a, b).

Moreover, the median T2 relaxation time corresponding to the T2 hyperintense regions on the T2 map was significantly higher (55.5 ms) than that of the relatively normal-appearing liver parenchyma (50 ms) (P = 0.030) (Figure 1c).

The median T1 relaxation time corresponding to the T2 hyperintense regions in both mapping techniques was significantly higher than that of the relatively normal-appearing liver parenchyma (Table 2) (Figure 1d-g). The RR of the T1 relaxation time in the region corresponding to the hyperintense areas on the T2WIs (50%) was significantly lower than that of the relatively preserved parenchyma (61%) on the MOLLI sequence images (P = 0.028). However, no significant difference was found in the RR (%) of the T1 relaxation time (67% vs. 68%) (P = 0.475) on the T1 map achieved using the B1-corrected VFA technique.

The adjusted postcontrast T1 values (MOLLI and B1-corrected VFA) corresponding to the T2 hyperintense regions were significantly lower (93.5 and 136 ms) than those of the relatively normal-appearing liver parenchyma (128 and 147 ms) (P = 0.028 and 0.024, respectively).

The median ADC value obtained from the areas corresponding to the hyperintense areas on the T2WIs was not statistically different from that obtained in the areas evaluated as relatively preserved ($1.167\ 10^{-3}$ vs. $0.969\ 10^{-3}\ mm^2/s$, P = 0.173).

Correlation between the quantitative magnetic resonance data and laboratory parameters, clinical scores, and prognostic indices

The median (minimum–maximum) values of the quantitative MR parameters measured from the entire cross-sectional surface of the liver are presented in Table 3.

Table 2. Comparison of the quantitative parameters of magnetic resonance elastography, T1 and T2 mapping, and the apparent diffusion coefficient in the caudate lobe vs. rest of the parenchyma and in areas seen as hyperintense on T2-weighted images vs. relatively preserved parenchyma

Parameters	Caudate lobe median (min–max)	Rest of parenchyma median (min–max)	*P*	T2 hyperintense areas median (min–max)	Relatively preserved parenchyma median (min–max)	*P*
Stiffness value (kPa)	3.29 (1.69–5.54)	5.07 (2.78–8.30)	0.001	6.14 (3.44–12.13)	2.96 (1.53–4.88)	0.001
Precontrast T1 value MOLLI 3(2)3(2)5*	778 (617–933)	867.5 (645–1.049)	0.012	1.105.5 (729–1.471)	699.5 (579–944)	0.012
Postcontrast T1 value MOLLI 3(2)3(2)5*	329 (198–419)	386 (225–452)	0.018	493 (298–798)	309 (163–416)	0.018
RR (%) MOLLI 3(2)3(2)5*	60 (40–71)	59 (38–65)	0.172	50 (34–62)	61 (36–77)	0.028
Adj. postcontrast T1 MOLLI 3(2)3(2)5*	120.5 (75–133)	112 (71–129)	0.027	93.5 (65–119)	128 (94–137)	0.028
Precontrast T1 value B1-corrected VFA	928 (525–1.111)	1,048 (655–1.347)	0.006	1,014 (643–1.791)	833 (598–1.008)	0.004
Postcontrast T1 value B1-corrected VFA	317 (157–481)	336 (151–567)	0.086	354 (151–820)	269 (136–429)	0.021
RR (%) B1-corrected VFA	67 (36–78)	66 (53–77)	0.399	67 (35–81)	68 (28–79)	0.475
Adj. postcontrast T1 B1-corrected VFA	140 (87–191)	136 (77–185)	0.058**	136 (82–177)	147 (91–201)	0.024
T2 value in FLASH*	54.5 (38–453)	54.5 (41–629)	0.141	55.5 (48–76)	50 (39–59)	0.030
ADC value (10^{-3} mm^2/s)	1.012 (0.891–2.041)	1.049 (0.910–1.294)	0.346	1.167 (0.853–1.847)	0.969 (0.851–1.505)	0.173

*, evaluated in 10 patients; **, marginally significant, T1 and T2 values are in ms; MOLLI, modified Look–Locker inversion recovery; RR, reduction rate; Adj, adjusted; VFA, variable flip angle; FLASH, fast low-angle shot; ADC, apparent diffusion coefficient.

No correlation was found between the whole liver stiffness values measured from the MR elastograms and the laboratory parameters/clinical scores and prognostic indices.

The platelet count was negatively correlated with the T1 relaxation time of the liver in the precontrast MOLLI sequence (r = –0.893, *P* = 0.007). A strong positive correlation was found between the Child–Pugh score and T1 relaxation times of the liver in both the precontrast MOLLI (r = 0.867, *P* = 0.012) and precontrast B1-corrected VFA (r = 0.621, *P* = 0.055) sequences. A strong positive correlation was identified between the direct bilirubin and T1 relaxation time in the precontrast B1-corrected VFA sequence (r = 0.703, *P* = 0.035).

The adjusted postcontrast T1 values showed a marginally significant, strong positive correlation with the AST level (r = 0.872, *P* = 0.054).

The Clichy score was positively correlated with the T1 relaxation time of the liver in the precontrast MOLLI sequence (r = 0.821, *P* = 0.023).

Table 3. Quantitative magnetic resonance parameters measured from the entire cross-sectional surface of the liver

Quantitative MR parameters	Median (min–max)
Stiffness value (kPa)	5.07 (2.78–8.30)
Precontrast T1 value* MOLLI 3(2)3(2)5	867.5 (645–1.049)
Postcontrast T1 value* MOLLI 3(2)3(2)5	386 (225–452)
Reduction rate (%)* MOLLI 3(2)3(2)5	59 (38–65)
Adjusted postcontrast T1 MOLLI 3(2)3(2)5*	112 (71–129)
Precontrast T1 value B1-corrected VFA	1.048 (655–1.347)
Postcontrast T1 value B1-corrected VFA	336 (151–567)
Reduction rate (%) B1-corrected VFA	66 (53–77)
Adjusted postcontrast T1 B1-corrected VFA	136 (77–185)
T2 value*	52.9 (41–62.9)

*, evaluated in 10 patients; MOLLI, modified Look–Locker inversion recovery; VFA, variable flip angle T1 and T2 values are in ms.

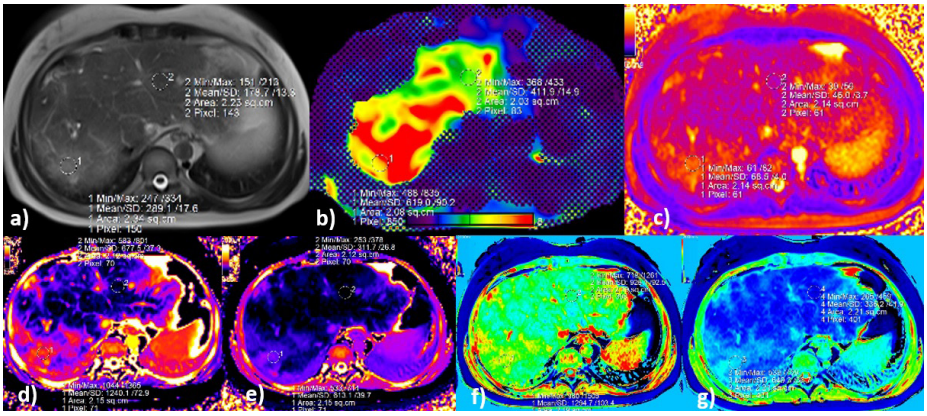

Figure 1. Magnetic resonance images acquired from a 32-year-old woman with occluded right and middle hepatic veins and a patent large left hepatic vein. **(a)** Axial T2-weighted image (T2WI), **(b)** color elastogram (confidence map), **(c)** T2 map, **(d)** pre-gadoxetic acid, and (e) post-gadoxetic acid T1 map acquired using the modified Look–Locker inversion (MOLLI) 3(2)3(2)5 sampling scheme, **(f)** pre-gadoxetic acid, and **(g)** post-gadoxetic acid B1-corrected variable flip angle (VFA) T1 map. All images were obtained at the same slice level. Regions of interest are drawn on the T2WIs **(a)** and copied and pasted onto the corresponding parametric maps **(b-g)**.

Axial T2WI (a) showing peripheral hyperintense tissue in segment VII, which corresponds to a region of confluent fibrosis. The numeric values are seen on the parametric maps. Compared with the relatively preserved left lobe parenchyma, fibrotic tissue has higher stiffness (4.1 vs. 6.1 kPa) **(b)**; longer T2 relaxation time (46 vs. 68 ms) **(c)**; and longer T1 relaxation times **(d)**; using the pre-gadoxetic acid T1 MOLLI technique (1.240 vs. 677 ms) **(e)**; and in the pre-gadoxetic acid B1-corrected VFA T1 map (1.294 vs. 926 ms) (f).

T1 relaxation times obtained from the fibrotic region and normal-appearing parenchyma using the post-gadoxetic acid T1 MOLLI technique **(e)** are 613 and 311 ms, respectively, and in the post-gadoxetic acid B1-corrected VFA T1 map **(f)** 649 and 336 ms, respectively. The reduction rate (%) of the T1 relaxation time in the area considered as fibrosis is significantly lower than that in the normal-appearing parenchyma at the hepatobiliary phase approximately 20 min after gadoxetic acid administration (fibrosis/relatively preserved parenchyma %; MOLLI technique 50%/54%, B1-corrected VFA T1 map 49%/63%).

No significant correlation was found between the MR parameters and Rotterdam index.

Serum creatinine levels exhibited a strong positive correlation with the T1 relaxation time of the liver in the postcontrast MOLLI sequence (r = 0.829, P = 0.042) and the precontrast (r = 0.661, P = 0.053) and postcontrast (r = 0.750, P = 0.052) B1-corrected VFA sequences. The RR was negatively correlated with the creatinine level (r = –0.943, P = 0.005), and the serum creatinine level had a strong positive correlation with the T2 relaxation time in the FLASH sequence (r = 0.857, P = 0.014). A strong negative relationship was identified between the serum sodium level and T1 relaxation time of the liver in the postcontrast MOLLI sequence (r = –0.928, P = 0.008).

Interobserver agreement

The ICC for all the measured parameters was excellent [ICC ≥ 0.911, (95% confidence interval, 0.651–0.981), P < 0.001].

Important qualitative findings observed on parametric magnetic resonance maps

In five patients, focal tissues that appeared normal on the T2WIs and T1 and T2 parametric maps were coded in yellow and/or red (indicating high stiffness) on the MREs (Figure 2). All of these patients (except one on which a contrast-enhanced examination could not be performed because of a previous history of a contrast media-related severe reaction) exhibited mottled parenchymal contrast enhancement, which is accepted as a manifestation of passive congestion of the liver.

In one patient, a segmental region, which seemed completely normal on the T2WI, exhibited abnormal findings when using mapping techniques and MRE.

Hepatocellular carcinoma was detected in two patients, and three patients, two of whom had undergone TIPS, had benign regenerative nodules in the liver.

Discussion

In the present study, quantitative MRI techniques enabled us to extract numeric data from parametric maps to assess of the parenchymal changes relative to normal-appearing (relatively preserved) tissues in BCS. Although the RR of the T1 relaxation time was not different, tissue stiffness and T1 relaxation values were lower in the caudate lobe than in the rest of the parenchyma, as expected. The ADC values, however, did not differ between normal-appearing and abnormal-appearing areas, including in the caudate lobe.

Edema and congestion, the important parenchymal alterations of acute BCS, are not prominent features in chronic BCS, as later stages are characterized by changes in fibrosis.[10] As BCS becomes chronic, T2 hyperintense areas become more prominent in the subcapsular regions of the liver. Since the BCS history of the study participants was longer than six months, we considered that such T2 hyperintense areas may reflect fibrosis caused by chronic BCS. Our results revealed that the T1 and T2 relaxation times were longer and stiffness values high in T2 hyperintense tissues compared with those of relatively preserved parenchyma (Table 2). The RR of the T1 relaxation time in the region corresponding to the hyperintense areas on the T2WIs (50%) was significantly lower than that in the other parts of the parenchyma (61%) on the MOLLI sequence images. High signal intensity characteristics on the T2WIs can be explained in part by the large water content of advanced fibrosis, which leads to prolonged T1 and T2 relaxation times.[13]

In addition to the staging of liver fibrosis, the potential role of elastography methods in assessing liver tissue stiffness has also been investigated in BCS.[14] Studies using ultrasound (US) elastography in BCS generally aim to evaluate parenchymal stiffness before and after vascular interventions. In these studies, a significant reduction in liver stiffness was found after treatment with balloon angioplasty.[15,16]

MRE is generally accepted as superior to US elastography because the latter has significant limitations, such as operator dependence and measurement difficulties, in cases of ascites and severe obesity.[17] Currently, there is a paucity of data in this context, and only two studies by the same author have reported MRE results in BCS.[18,19] The

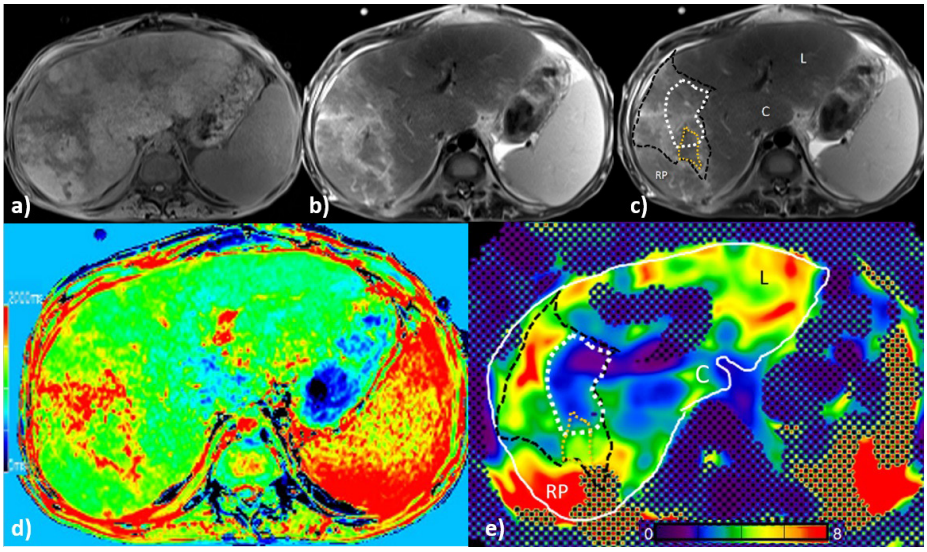

Figure 2. Magnetic resonance (MR) images acquired from a 24-year-old man with occluded right and middle hepatic veins and inferior vena cava. **(a)** Axial T1-weighted image (T1WI), **(b, c)** axial T2-weighted images (T2WIs), **(d)** native B1-corrected variable flip angle (VFA) T1 map, and **(e)** color elastogram (confidence map). All images are obtained at the same slice level.

T1WI **(a)** and T2WI **(b)** show peripheral mass-like tissue change, mainly located in the lateral aspect of the right lobe, with relatively sharp but irregular borders. This area, thought to be confluent fibrosis, is shown in **(c)** with its borders drawn in black. On the color B1-corrected VFA T1 map **(d)**, the tissue in question is encoded with red and the T1 relaxation time is long. On T2WI **(c)**, the medial part of the hyperintense area, which looks like a continuation of fibrosis (white outline), is encoded with blue in the MR elastogram **(e)**; its stiffness values are not high enough to suggest fibrosis. By contrast, the area that appears normal compared with its surroundings (yellow outline) on the T2WI **(c)**, the posterior subcapsular region in the right lobe, and the majority of the left hepatic lobe (L), are encoded with yellow and red in the MR elastogram, indicating high stiffness values. In the areas described, the possibility of congestion, which increases tissue stiffness, should be considered. Note also the relatively normal appearance of the caudate lobe **(c)**, with normal signal intensity on conventional sequences **(a, b)** and blue encoding (normal) on the MR elastogram and B1-corrected VFA T1 map.

authors concluded that segmental stiffness measured through an MRE was a promising reproducible quantitative biomarker for monitoring the treatment response to endovascular intervention in patients with BCS.[18] In the second study, the authors suggested that using an MRE for liver stiffness measurements was effective for evaluating liver function in BCS.[19] However, none of the laboratory parameters and indices appeared to correlate with the liver stiffness values in our study. This may be due to the small sample size.

Although fibrosis could not be definitively excluded in the studies mentioned above performed using US and MRE, studies suggest that the increase in tissue stiffness seen in BCS is the result of congestion rather than fibrosis.[18-20] Hepatic congestion, which can spuriously increase liver stiffness measurements, may be differentiated from fibrosis through conventional imaging, clinical information, and liver function test results.[7] With the onset of clinical findings, the hepatic mottled enhancement in the portal venous phase of dynamic contrast-enhanced imaging reflects portal stasis and, indirectly, hepatic congestion.[21] Sluggish flow, which can cause increased blood volume (congestion) in the portal vessels and sinusoids, is expected to develop in the early stages, but it can also be seen in the "acute on chronic" form of the disease with clinical exacerbation. The thrombotic extension could play a role in this scenario.[22]

Estimating the hepatic functional reserve is important for the prognosis and management of patients with BCS. An essential but unanswered issue in BCS is how to take the degree of liver dysfunction into account when choosing the type of therapy.[1] In routine clinical practice, liver function in BCS is often determined using clinical signs and biochemical blood parameters.[23] However, the measurement of biochemical parameters provides only indirect information about hepatocyte injury. As individual segments are drained by unique hepatic vein branches, the development of hepatocyte damage is expected to be limited mainly to the region drained by the occluded vessel. Liver function tests may fail to detect this topographic segmental dysfunction. Although regional non-enhancement on dynamic imaging may indicate hepatocyte damage,[24] having a direct measurement of hepatocyte function is desirable. In this context, T1 mapping techniques are increasingly used in the medical arena to provide an objective observation of the damaged areas in the liver.[25]

In our case series, we used gadoxetic acid-enhanced MRI to objectively evaluate global and regional liver function. The hepatic elimination of gadoxetic acid is dependent on the integrity of the hepatocyte mass. The uptake of the contrast medium by the hepatocytes allows a quantitative estimation of segmental liver function on parametric maps. T1 mapping of the liver can enable an evaluation of liver function by using precontrast and postcontrast HB phase images and the RR of T1 relaxation times (normally above 60%).[26,27] Approximately 20 min after intravenous gadoxetic acid administration, we found that the RR of the T1 relaxation time was significantly lower than that of normal-appearing (relatively preserved) parenchyma because of the reduced hepatocyte uptake in the areas considered as fibrosis (50% vs. 61% in the MOLLI technique).

Several prognostic indices have been described to predict outcomes in BCS, including the Child–Pugh score, Clichy index, and Rotterdam index.[9,28] We investigated the possible correlation between these three indices and quantitative MR parameters, revealing that the Child–Pugh score and serum creatinine level, which are important determinants of prognosis, were correlated with the T1 relaxation time of the liver. Patients with reduced liver function had longer precontrast T1 relaxation times when classified by the Child–Pugh score, which correlated positively with the progression of liver damage. The Clichy score was also positively correlated with the T1 relaxation time of the liver in the precontrast MOLLI sequence.

Renal failure secondary to liver parenchyma disease is usually functional and occurs in the absence of significant changes in renal histology.[29] In our case series, interestingly, we found that serum creatinine values exhibited a positive correlation with the T1 values obtained from precontrast and postcontrast T1 and T2 maps. Creatinine levels were also negatively correlated with the RR of the T1 relaxation time. In the study by Zeitoun et al.[30], serum creatinine was identified as one of the four significant prognostic factors in a multivariate analysis of BCS patients. How-

ever, the creatinine levels of the patients in this study were within the normal range (0.40–1.34 mg/dL), indicating that although the correlation was statistically significant, it was not clinically significant in these cases, or at least not at this stage.

This study has several limitations. First, the sample size is small, which negatively affects the generalization of our findings; the low incidence of the disease in the general population is responsible for this limitation. However, because the condition is rare, the findings of this study offer new potentially useful information for this patient population. A larger number of patients, some in the acute stage, would have allowed us to make a more detailed evaluation. Second, this study has some inherent limitations because of its retrospective design, resulting in incomplete data (relaxation times obtained from electrocardiogram-gated T1 MOLLI and T2 maps) in four patients. Third, three of our patients had undergone TIPS, which may have led to a decrease in the MRE stiffness values. However, because these patients were in the chronic stage and we focused on relatively long-term parenchymal changes, we did not exclude these patients. We considered that except for minor tissue changes, any damage that appeared resulted in some degree of fibrosis. Fourth, we hypothesized that subcapsular hyperintensities in T2WIs were fibrosis (as detailed in the literature, i.e., in[13]), and in the present study, we identified a prolongation of both T1 and T2 relaxation times and increased stiffness values. An important limitation of our study is that the presence of fibrosis was not confirmed histopathologically. In five patients, we observed that focal tissues that appeared normal on the T2WIs and T1 and T2 parametric maps were coded in yellow and/or red (indicating high stiffness) on MR the elastograms. Mottled contrast enhancement was observed in these cases. Hepatic congestion (increased upload) was not distributed homogeneously, as can be inferred from multiparametric techniques and different parametric maps. We hypothesize that fibrotic tissues, in addition to their high stiffness in the MREs, display pathological appearance, both visually and quantitatively, relative to the rest of the parenchyma on the T1 maps. In this context, we believe that tissues that are stiff in the MRE but appear normal on the T2WIs and T1 maps might be congested. The combined use of T2WIs, T1 mapping, and MREs (i.e., a multiparametric MR approach) can be expedient to further understand the pathophysiology.

In conclusion, the relative shortening of the T1 relaxation time in the HB phase after hepatocyte-specific contrast administration allows for the quantitative evaluation of global and segmental liver function in BCS. By providing absolute and comparable data, T1 relaxation times can be used to estimate the heterogeneous distribution of liver function in patients with BCS. However, T2 mapping and ADC values do not significantly contribute to the quantitative assessment of tissue changes. In this syndrome, in addition to fibrosis, hepatic congestion and sinusoidal dilatation appear to be responsible for elevated tissue stiffness. In the follow-up of these patients, quantitative parameters obtained from MRE and T1 mapping techniques, along with laboratory and clinical parameters, may allow an objective temporal evaluation of segmental and global changes. An alteration in quantitative parameters over time with the progression of the chronic process may be used to predict the course of the disease. The T1 relaxation time has the potential to be an objective prognostic marker because it reveals a correlation with important prognostic determinants such as the Child–Pugh score and serum creatinine level. To establish the role of quantitative MR methods in BCS, further prospective studies with large sample sizes are required. We hope our study promotes further methodologic work to determine clinically important differences in BCS.

Conflict of interest disclosure

The authors declared no conflicts of interest.

References

1. Janssen HL, Garcia-Pagan JC, et al. Budd-Chiari syndrome: a review by an expert panel. *J Hepatol.* 2003;38(3):364-371. [CrossRef]
2. Valla DC. The diagnosis and management of the Budd-Chiari syndrome: consensus and controversies. *Hepatology.* 2003;38(4):793-803. [CrossRef]
3. Plompen EPC, Darwish Murad S, Hansen BE, et al. Prothrombotic genetic risk factors are associated with an increased risk of liver fibrosis in the general population: the Rotterdam study. *J Hepatol.* 2015;63(6):1459-1465. [CrossRef]
4. Xu P, Lyu L, Sami MU, et al. Diagnostic accuracy of magnetic resonance angiography for Budd-Chiari syndrome: a meta-analysis. *Exp Ther Med.* 2018;16(6):4873-4878. [CrossRef]
5. Li Q, Chen T, Shi N, Ye W, Yuan M, Shi Y. Quantitative evaluation of hepatic fibrosis by fibro Scan and Gd-EOB-DTPA-enhanced T1 mapping magnetic resonance imaging in chronic hepatitis B. *Abdom Radiol (NY).* 2022;47(2):684-692. [CrossRef]
6. Simonetto DA, Yang HY, Yin M, et al. Chronic passive venous congestion drives hepatic fibrogenesis via sinusoidal thrombosis and mechanical forces. *Hepatology.* 2015;61(2):648-659. [CrossRef]
7. Idilman IS, Li J, Yin M, Venkatesh SK. MR elastography of liver: current status and future perspectives. *Abdom Radiol (NY).* 2020;45(11):3444-3462. [CrossRef]
8. Cazals-Hatem D, Vilgrain V, Genin P, et al. Arterial and portal circulation and parenchymal changes in Budd-Chiari syndrome: a study in 17 explanted livers. *Hepatology.* 2003;37(3):510-519. [CrossRef]
9. Sakr M, Abdelhakam SM, Elsayed SA, et al. Validation of prognostic indices in Egyptian Budd-Chiari syndrome patients: a single-center study. *World J Gastroenterol.* 2017;23(4):629-637. [CrossRef]
10. Noone TC, Semelka RC, Siegelman ES, et al. Budd-Chiari syndrome: spectrum of appearances of acute, subacute, and chronic disease with magnetic resonance imaging. *J Magn Reson Imaging.* 2000;11(1):44-50. [CrossRef]
11. Katsube T, Okada M, Kumano S, et al. Estimation of liver function using T1 mapping on Gd-EOB-DTPA-enhanced magnetic resonance imaging. *Invest Radiol.* 2011;46(4):277-283. Erratum in: *Invest Radiol.* 2013;48(2):112. [CrossRef]
12. Yoon JH, Lee JM, Paek M, Han JK, Choi BI. Quantitative assessment of hepatic function: modified look-locker inversion recovery (MOLLI) sequence for T1 mapping on Gd-EOB-DTPA-enhanced liver MR imaging. *Eur Radiol.* 2016;26(6):1775-1782. [CrossRef]
13. Faria SC, Ganesan K, Mwangi I, et al. MR imaging of liver fibrosis: current state of the art. *Radiographics.* 2009;29(6):1615-1635. [CrossRef]
14. Ferraioli G, Barr R. Ultrasound liver elastography beyond liver fibrosis assessment. *World J Gastroenterol.* 2020;26(24):3413-3420. [CrossRef]
15. Mukund A, Pargewar SS, Desai SN, Rajesh S, Sarin SK. Changes in liver congestion in patients with Budd-Chiari syndrome following endovascular ınterventions: assessment with transient elastography. *J Vasc Interv Radiol.* 2017;28(5):683-687. [CrossRef]
16. Wang HW, Shi HN, Cheng J, Xie F, Luo YK, Tang J. Real-time shear wave elastography (SWE) assessment of short- and long-term treatment outcome in Budd-Chiari syndrome: a pilot study. *PLoS One.* 2018;13(5):e0197550. [CrossRef]
17. Srinivasa Babu A, Wells ML, Teytelboym OM, et al. Elastography in chronic liver disease: modalities, techniques, limitations, and future directions. *Radiographics.* 2016;36(7):1987-2006. [CrossRef]

18. Xu P, Lyu L, Ge H, et al. Segmental liver stiffness evaluated with magnetic resonance elastography ıs responsive to endovascular ıntervention in patients with Budd-Chiari syndrome. *Korean J Radiol.* 2019;20(5):773-780. [CrossRef]
19. Xu P, Lyu L, Lu X, Hu C, Xu K. Evaluating the short-term clinical efficacy of magnetic resonance elastography in patients with Budd-Chiari syndrome. *Acad Radiol.* 2021;28(Suppl 1):S179-S183. [CrossRef]
20. Mukund A, Sarin SK. Budd-Chiari syndrome: a focussed and collaborative approach. *Hepatol Int.* 2018;12(6):483-486. [CrossRef]
21. Erden A, Erden I, Yurdaydin C, Karayalçin S. Hepatic outflow obstruction: enhancement patterns of the liver on MR angiography. *Eur J Radiol.* 2003;48(2):203-208. [CrossRef]
22. Mancuso A. An update on management of Budd-Chiari syndrome: the issues of timing and choice of treatment. *Eur J Gastroenterol Hepatol.* 2015;27(3):200-203. [CrossRef]
23. Coilly A, Potier P, Broué P, et al. Budd-Chiari syndrome. *Clin Res Hepatol Gastroenterol.* 2020;44(4):420-425. [CrossRef]
24. Erden A, Erden I, Karayalçin S, Yurdaydin C. Budd-Chiari syndrome: evaluation with multiphase contrast-enhanced three-dimensional MR angiography. *AJR Am J Roentgenol.* 2002;179(5):1287-1292. [CrossRef]
25. Nilsson H, Blomqvist L, Douglas L, et al. Dynamic gadoxetate-enhanced MRI for the assessment of total and segmental liver function and volume in primary sclerosing cholangitis. *J Magn Reson Imaging.* 2014;39(4):879-886. [CrossRef]
26. Kamimura K, Fukukura Y, Yoneyama T, et al. Quantitative evaluation of liver function with T1 relaxation time index on gadoxetic acid-enhanced MRI: comparison with signal intensity-based indices. *J Magn Reson Imaging.* 2014;40(4):884-889. [CrossRef]
27. Haimerl M, Verloh N, Zeman F, et al. Assessment of clinical signs of liver cirrhosis using T1 mapping on gadoxetic acid-enhanced 3T MRI. *PLoS One.* 2013;8(12):e85658. [CrossRef]
28. Qi X, Ren W, Wang Y, Guo X, Fan D. Survival and prognostic indicators in Budd-Chiari syndrome: a systematic review of 79 studies. *Expert Rev Gastroenterol Hepatol.* 2015;9(6):856-875. [CrossRef]
29. Fortune B, Cardenas A. Ascites, refractory ascites and hyponatremia in cirrhosis. *Gastroenterol Rep (Oxf).* 2017;5(2):104-112. [CrossRef]
30. Zeitoun G, Escolano S, Hadengue A, et al. Outcome of Budd Chiari syndrome: a multivariate analysis of factors related to survival including surgical portosystemic shunting. *Hepatology.* 1999;30(1):84-89. [CrossRef]